An Anomalous Enhancement of the $A_g(2)$ Mode in the Resonance Raman Spectra of C_{60} Embedded in Single-Walled Carbon Nanotubes during Anodic Charging

Martin Kalbac,*,† Viktor Zólyomi,‡,§ Ádám Rusznyák,|| János Koltai,|| Jenő Kürti,|| and Ladislav Kavan†

J. Heyrovský Institute of Physical Chemistry, Academy of Sciences of the Czech Republic, v.v.i., Dolejškova 3, CZ-18223 Prague 8, Czech Republic, Physics Department, Lancaster University, Lancaster, LA1 4YB, United Kingdom, Research Institute for Solid State Physics and Optics of the Hungarian Academy of Sciences, Konkoly-Thege M. út 29-33, H-1121 Budapest, Hungary, and Department of Biological Physics, Eötvös Loránd University, Pázmány Péter sétány 1/A H-1117 Budapest, Hungary

Received: October 29, 2009; Revised Manuscript Received: January 8, 2010

The effect of electrochemical charging on C_{60} fullerenes embedded in single-walled carbon nanotubes (peapods) has been studied. The Raman $A_g(2)$ mode of C_{60} fullerene has been used as a probe. The spectra were measured using seven different laser excitation energies. For cathodic charging we observed bleaching of the $A_g(2)$ mode independent of laser excitation energy. On the other hand for anodic charging the behavior of the $A_g(2)$ mode was dependent on laser excitation energy. The intensity of the $A_g(2)$ mode decreased only for the 1.16 eV laser excitation energy. In the case of other laser excitation energies (2.70, 2.60, 2.54, 2.41, 2.33, 2.18 eV) an increase of intensity has been observed. The dependence of the slope of the intensity on the electrode potential has been found to be a function of laser excitation energy. Observation of the upshift of the $A_g(2)$ frequency supported by first principles calculations suggests that only a small amount of charge penetrates the nanotube, resulting in partial charge on the encapsulated fullerenes.

Introduction

The filling of the inner space of single-walled carbon nanotubes (SWCNTs) with other molecules is a challenging topic in materials research since the interaction of components in this nanoassembly may lead to novel and attractive properties.[1] Furthermore, the species confined in the inner space of a nanotube are forced to assemble in one dimension. They are also protected from the environment; therefore, structures which are very reactive might be stabilized inside a carbon nanotube. Recently, several different materials were successfully encapsulated in the inner space of SWCNTs[1] including organic molecules,[2] inorganic salts,[3] fullerenes,[4] and even narrow SWCNTs.[5] To increase the benefit from the encapsulated structures, it is desirable to have a possibility to modify the properties of the species inside carbon nanotubes.[6] An efficient approach to modify the electronic structure of molecules inside carbon nanotubes is doping.[7,8] This can be realized either by treatment of carbon nanostructures with redox active molecules or by electrochemical charging. However, in several cases the chemical dopant can penetrate into the SWCNT and react directly with the encapsulated species.[9−13] A chemical doping is highly irreversible, and in some cases the chemical dopant cannot be removed even by extraction with solvent.[10−12] The doped intratubular species can even assist the coalescence of the C_{60} molecules inside SWCNTs.[14] Electrochemical charging in electrolyte solutions, on the other hand, mimics a double layer capacitor,[15] where the charge carriers are injected into the nanotube from the electrode support and the electrolyte ions compensate the injected charge.[15] For aqueous electrolyte solutions and high electrode potentials, some irreversible changes of SWCNTs in addition to reversible double layer charging may also be observed.[16,17] In contrast, the electrochemical charging in nonaqueous electrolyte solutions allows charging in a relatively wide range of potentials where no irreversible changes are induced.[15] Therefore the electrochemical charging in nonaqueous electrolyte solutions is the most convenient method for studies of doping behavior and the electronic properties of carbon nanostructures. This has been demonstrated by a number of detailed studies on SWCNTs which paved the way for understanding of the mechanism of the change of electronic structure which occurs during doping.[15,18,19] It has been shown that the filling/depleting of Van Hove singularities with electrons has important consequences for the whole electronic structure.[18] It has also been confirmed that the electrochemically induced changes in the SWCNT electronic structure influence the embedded species. For example it was shown experimentally that it is possible to modify the electronic structures of inner tubes in double-walled carbon nanotubes (DWCNTs),[20,21] and intratubular molecules such as C_{60},[8,22] C_{70},[8] or even $Dy_3N@C_{80}$.[23] The studies of C_{60} inside SWCNTs are of great importance, since the doping dependence of Raman frequencies of the C_{60} is known in detail.[24−27] In particular, the Raman shift of the pentagonal pinch mode, $A_g(2)$, is very important since this line is relatively strong and its frequency scales linearly with the applied charge during electron injection.[26] Therefore the $A_g(2)$ mode can be used as a marker for evaluation of the charge transfer processes in C_{60}@SWCNTs. This has been shown on the example of doping of fullerene peapods with alkali metals.[9,10]

* To whom correspondence should be addressed. Tel: 420 2 6605 3804. Fax: 420 2 8658 2307. E-mail: kalbac@jh-inst.cas.cz.

† J. Heyrovský Institute of Physical Chemistry, Academy of Sciences of the Czech Republic.

‡ Physics Department, Lancaster University.

§ Research Institute for Solid State Physics and Optics of the Hungarian Academy of Sciences.

|| Eötvös Loránd University.

10.1021/jp9103273
Published on Web 01/25/2010

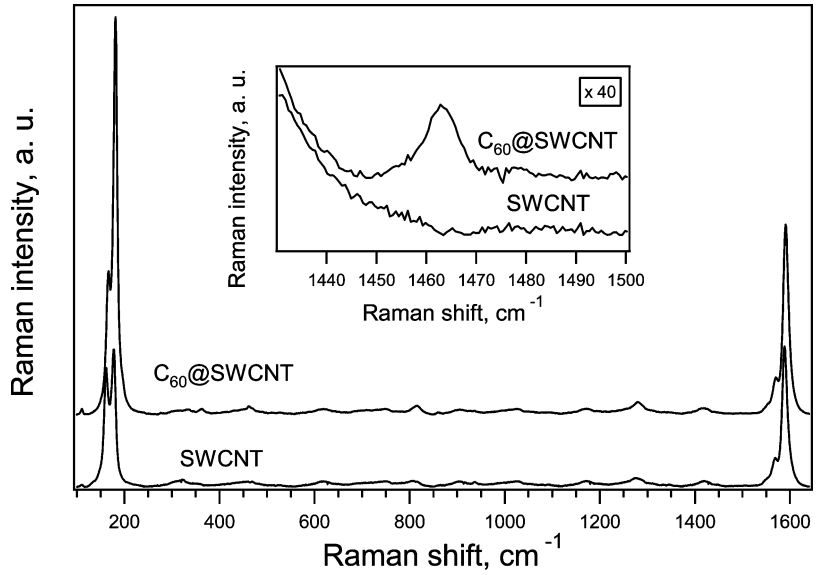

Figure 1. The Raman spectra of SWCNTs and C_{60}@SWCNT measured using the 1.16 eV laser excitation energy. The inset shows the region of the $A_g(2)$ mode of the C_{60} fullerene. The intensity scale is zoomed by a factor of 40.

Despite the fact that numerous studies have dealt with the doping of inner species inside SWCNTs, open questions still persist. One of the least understood issues is the enhancement of the Raman signal of C_{60} fullerene modes in peapods at positive potentials (the so-called "anodic Raman enhancement")[8] which is not reproduced for C_{70} peapods[8] nor for inner tubes of DWCNTs.[20,28] Here, we present a detailed in situ Raman spectroelectrochemical study of the C_{60} inside SWCNTs (C_{60}@SWCNT). We experimentally show that the $A_g(2)$ fullerene mode is sensitive not only to the electrochemical charge but also to the laser excitation energy. This is demonstrated by a careful analysis of the $A_g(2)$ mode during electrochemical charging using seven different laser excitation energies and electrode potentials between −1.5 and +1.5 V. A theoretical discussion of the Raman shift and its dependence on the charging level is also presented.

Results and Discussion

Figure 1 shows the Raman spectra of SWCNTs and C_{60}@SWCNT measured using 1.16 eV laser excitation energy. The spectra are dominated by the nanotube radial breathing mode (RBM) at about 180 cm^{-1} and tangential displacement mode (TG) bands at about 1590 cm^{-1}, respectively. A detailed view of the $A_g(2)$ mode region is shown as an inset in Figure 1. For C_{60}@SWCNT, the $A_g(2)$ mode of the C_{60} fullerene is at 1464 cm^{-1}. The position of the band is slightly downshifted with respect to that in the free fullerene as a consequence of encapsulation. The encapsulation also affects the Raman bands of the carbon nanotube through the interaction between the tube and the fullerenes. Hence, some small shifts of the RBM bands and slightly modified resonance condition can be rationalized.[29]

The Raman spectra of C_{60}@SWCNT measured in situ at different potentials are shown in Figure 2. The spectra are displayed in the region of dominating nanotube bands: the RBM (left panel) and the TG (right panel). Increasing the magnitude of the electrode potential leads to the bleaching of both nanotube modes independently of the sign of the potential. This observation was previously interpreted as a result of gradual filling/depleting of Van Hove singularities which are employed in the resonance enhancement of the Raman signal.[15,30] More recently, we have shown that filling of any electronic states causes perturbation of the whole electronic structure of the carbon nanotubes.[18,31] Hence, the bleaching starts by filling/depleting of the first pair of electronic states independently of its involvement in the resonance enhancement. However, the bleaching behavior caused by filling/depleting of electronic states, which are not in resonance with the particular laser excitation energy is different from that caused by filling/depleting electronic states, which are in resonance as has been shown by the detailed study of the (6,5) nanotubes.[32] Therefore the response of the Raman spectra to the electrochemical doping is relatively complex, but careful evaluation of the Raman data gives access to detailed information about the electronic structure of carbon nanostructures in a relatively wide range of potentials.

The Raman signal of the fullerene modes in C_{60}@SWCNT is very weak compared to the signal of the nanotube modes (the RBM and the TG modes); thus it is not distinguished in Figure 2. In Figure 3 we show zoomed detail of the potential-dependent Raman spectra of C_{60}@SWCNT, where the $A_g(2)$ fullerene mode occurs. The intensity of the $A_g(2)$ mode is obviously a function of electrode potential. The intensity of the $A_g(2)$ mode is attenuated when the magnitude of the electrode potential increases or decreases. This is similar to the behavior of nanotube modes. However, it is the first time the bleaching of the $A_g(2)$ mode has been observed for both cathodic and anodic doping. In previous studies the intensity of the $A_g(2)$ mode decreased at cathodic potentials but increased during anodic charging.[8,22]

The change of the intensity of the $A_g(2)$ mode with the applied potential was reversible. We measured the Raman spectra of C_{60}@SWCNT at 0 V after multiple potential cycles, and we did not observe significant intensity change of the $A_g(2)$ mode. This confirms that if the C_{60} is protected by a nanotube wall, it is more stable in the laser light than unprotected C_{60}. It is also a sign that our material does not contain free C_{60} molecules, since they would be destroyed during our measurements and the signal intensity of the $A_g(2)$ mode would be reduced.[33] The presence of free C_{60} outside the SWCNT in our sample is not very likely, because free molecules are removed during the peapods synthesis. Moreover, free C_{60} would exhibit the $A_g(2)$ line at ca. 1468 cm^{-1},[33] but in our case, this peak was located

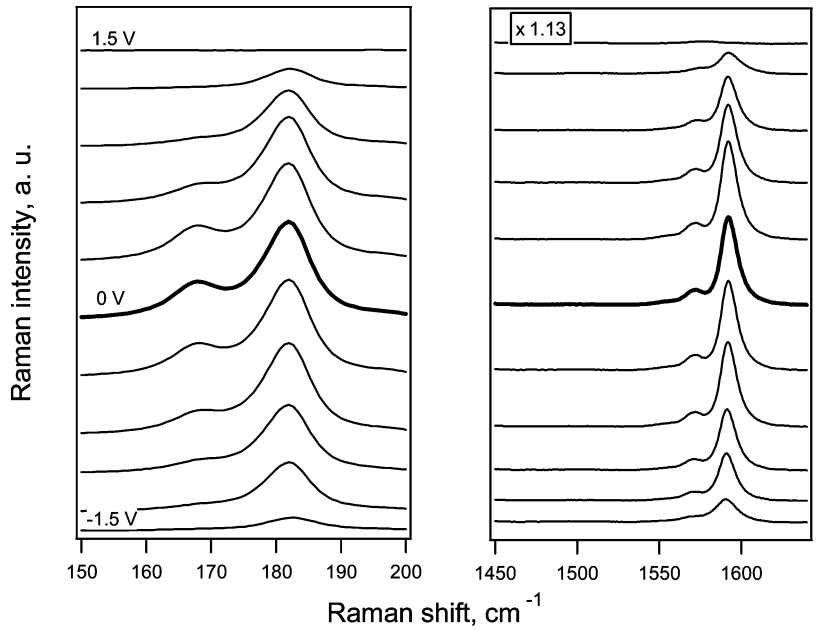

Figure 2. In situ Raman spectroelectrochemical data on C_{60}@SWCNT measured using the 1.16 eV laser excitation energy. The electrode potential was changed in the range from −1.5 to 1.5 V (from bottom to top) with a step of 0.3 V.

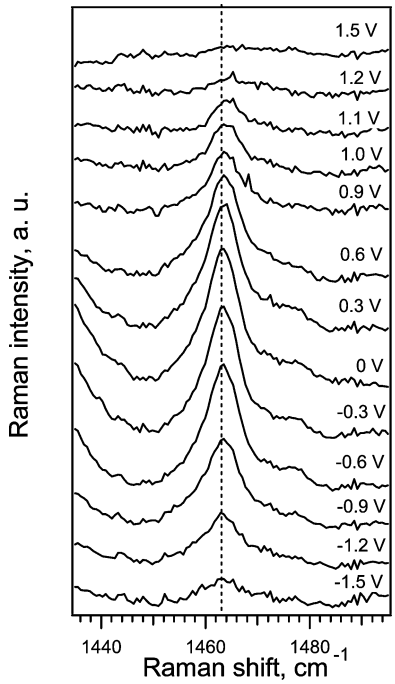

Figure 3. The development of the $A_g(2)$ mode in the Raman spectra of C_{60}@SWCNT in dependence on electrode potential. The spectra are excited using 1.16 eV laser excitation energy. The dashed line corresponds to the frequency of the $A_g(2)$ mode at 0 V.

at 1464 cm^{-1} without any clear evidence for a blue-shifted component of a free molecule.

An example of anodic enhancement of the $A_g(2)$ mode in the Raman spectra is shown in Figure 4. Here, the Raman spectra were excited by 2.70 eV laser excitation energy. Obviously for negative doping the $A_g(2)$ mode intensity is decreasing similarly as observed for the 1.16 eV laser excitation shown in Figure 3. However, for positive potentials, the signal is strongly enhanced. At the maximum applied positive potential (1.5 V) the signal is about 1.5 times stronger than that at 0 V. The $A_g(2)$ mode also shifts its position to higher frequencies at anodic doping and slightly downshifts for negative doping. This is consistent with results obtained from chemical doping of fullerene peapods: negative chemical doping leads to a downshift in dependence on the amount of charge transferred to the fullerene.[34] The experimental data on chemical oxidation of fullerenes inside SWCNTs are not available, but simple extrapolation of the dependence found for negative doping would explain an upshift of the $A_g(2)$ mode during positive charging. More careful analysis of the $A_g(2)$ mode shows that the dominant peak at 1464 cm^{-1} has a less intensive shoulder downshifted by about 5 cm^{-1}. This shoulder is frequently observed in C_{60} peapods, and it is explained by molecular-dynamics simulations which show that the two bands emerge from a coupling of the C_{60} totally symmetric modes to the fullerene translational mobility inside the tube. The doublet is thus suggested to be the spectroscopic fingerprint of different mobilities of C_{60} fullerenes in the tubes.[35]

We note, that a similar frequency shift also occurs for 1.16 eV laser energy excitation, but the intensity of the $A_g(2)$ mode is strongly bleached at high electrode potentials. Nevertheless, one can trace a little upshift of the band between 0.9 and 1.2 V, which is consistent with measurement using other laser excitation lines. A more detailed discussion of the frequency shifts of the $A_g(2)$ mode is given later in this section.

The changes of the Raman intensity with dependence on electrode potential are obviously a function of the laser excitation energy. Figure 5 shows the summarized plot of the integrated $A_g(2)$ mode Raman intensity $I(A_g(2))$ vs electrode potential for 1.16 and 2.70 eV and a further five different laser excitation energies (2.60, 2.54, 2.41, 2.33, 2.18 eV). For convenience the $I(A_g(2))$ values at different potentials are normalized to the $I(A_g(2))$ value at the potential of 0 V.

The plot also clearly demonstrates the asymmetry in the behavior of the $I(A_g(2))$ on electrode potential with respect to positive and negative values. For negative potentials the $I(A_g(2))$ is attenuated as the magnitude of the electrode potential is increased independently of laser excitation energies. On the other hand for positive doping, the $I(A_g(2))$ vs electrode potential profiles are significantly dependent on laser excitation energy. The strongest increase of intensity was observed for laser excitations between 2.33 and 2.60 eV, where at the maximum

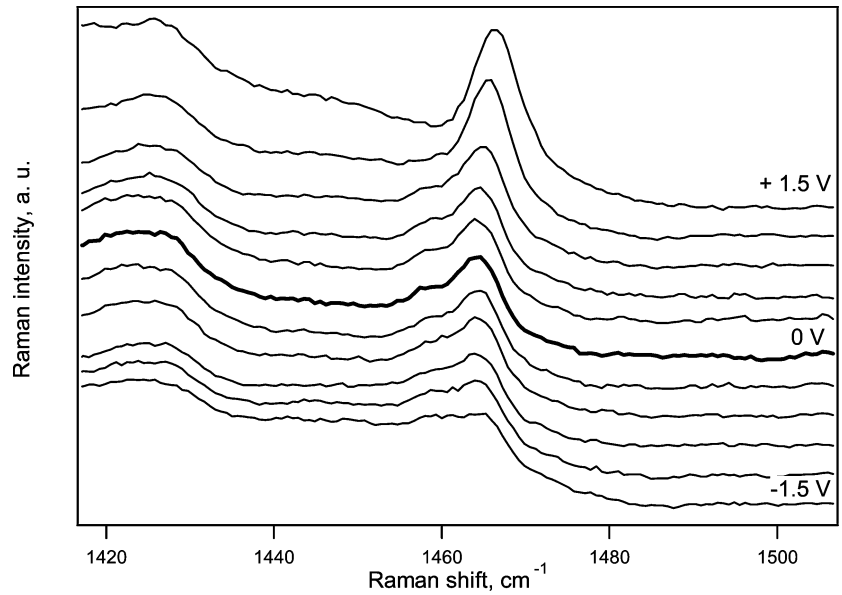

Figure 4. The development of the $A_g(2)$ mode in the Raman spectra of C_{60}@SWCNT and dependence on electrode potential. The spectra are excited with 2.70 eV laser energy. The electrode potential was changed in the range from −1.5 to 1.5 V (from bottom to top) with a 0.3 V step.

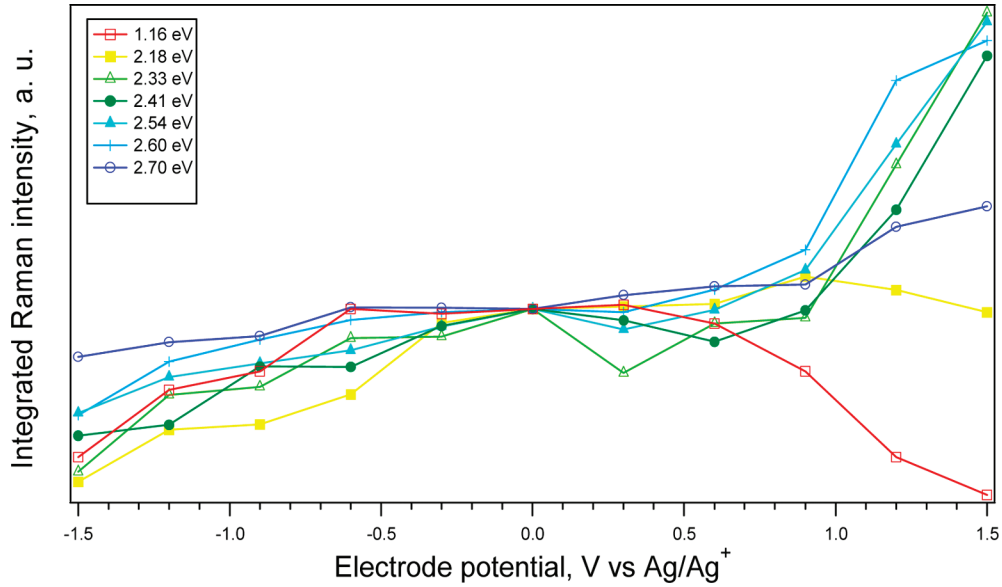

Figure 5. Normalized integrated Raman intensity of the $A_g(2)$ mode at different electrode potentials. The spectra were excited by 2.70, 2.60, 2.54, 2.41, 2.33, 2.18, and 1.16 eV laser energies as indicated in the figure. The solid lines serve as guides for the eye.

applied positive potential (1.5 V) the integrated Raman signal $I(A_g(2))$ is about 2.5 times stronger than that at 0 V. On the other hand, only a small increase in intensity was found in the case of the 2.18 eV laser excitation energy. A decrease of $I(A_g(2))$ during positive doping was observed only for the 1.16 eV laser excitation energy. In other words the slope of the $I(A_g(2))$ enhancement at anodic potentials increases and then again decreases by changing the laser excitation energy from 2.70 to 1.16 eV.

It should be noted that there is also an offset in the intensity enhancement/bleaching of the $A_g(2)$ mode. The $I(A_g(2))$ does not change within a potential window of ca. ±0.6 V. On the other hand at potentials higher/smaller than ca. ±0.6 V, the $I(A_g(2))$ is bleached/enhanced significantly. The offset is clearer for positive potentials, where the changes are more pronounced.

The reason for the anodic enhancement of the $I(A_g(2))$ was not fully explained up to now. This effect is unique for C_{60} peapods, and it was never found for peapods with other fullerenes (C_{70}, $Dy_3N@C_{82}$).[8,23] In our previous studies on DWCNTs, we have shown that the electrochemical charging of the DWCNTs causes bleaching of the signal of both outer and inner tubes for positive and negative potentials.[20,21,36] Therefore the inner tubes are experiencing the effects of charging. Nevertheless, there is a delay in the bleaching behavior of inner tubes, which indicates different amounts of charges located on inner and outer tubes, respectively. A similar effect may be expected for encapsulated fullerenes; hence we assume that the fullerene molecules are in fact charged as a result of electrochemical treatment, albeit the charge is most likely very small due to the screening effect caused by the nanotube.

The dependence of $I(A_g(2))$ vs electrode potential profiles on laser excitation energy is a new phenomenon observed here for the first time. The reason for this effect is not understood yet. In principle there are two possible explanations: (1) the

change of the optical "transparency" of the tube and (2) the change of electronic structure of fullerene, which leads to the stronger/weaker Raman resonance effect. The change of the transparency of the nanotubes due to removal of electrons does not seem to be the reason for the observed effects. This is because the enhancement has been so far observed only in the case of C_{60}. For example in the case of C_{70} peapods, only bleaching of the Raman modes with increasing magnitude of electrode potential has been observed.[8] Hence, the effect is obviously dependent on the encapsulated species. Furthermore the intensity of enhancement is dependent on laser excitation energy. Assuming a change of transparency of SWCNT due to the change in the electrode potential, it should be observed for any laser excitation energy.

Therefore the change of the electronic structure of the C_{60} fullerene seems to be the more probable reason for dependence of the intensity $I(A_g(2))$ vs electrode potential profiles on laser excitation energy; i.e., it is a resonance effect. The absorption of the C_{60} fullerene in the region probed by lasers in this study (1.9−2.8 eV) corresponds to forbidden singlet−singlet transitions, which are enabled by Jahn−Teller (JT) dynamic distortions.[37] The enhancement of $I(A_g(2))$ in the Raman spectra is observed for the laser within the interval 2.18−2.7 eV, which overlaps the fullerene absorption band.[27] This is also consistent with a study on pristine C_{60}, where resonance Raman spectra showed maximum enhancement for the 3.00 eV laser energy excitation.[25] On the other hand the attenuation of the $I(A_g(2))$ is observed for 1.16 eV. At this energy there is no optical absorption in C_{60}. A more detailed analysis of Figure 5 shows that the maximum enhancement of $I(A_g(2))$ in the Raman spectra does not correspond to the maximum in the C_{60} fullerene absorption spectrum.[27] Furthermore, the spectra of C_{60}^+ and C_{60}^- exhibit a significant absorption band around 1 eV,[27] which is not present in neutral C_{60}. This is contrary to our observation since no enhancement of the signal was found in the spectra excited by 1.16 eV laser excitation energy. Nevertheless, the reported absorption spectra were measured for fullerene in solution. For a one-dimensional row of fullerenes in the environment of SWCNTs, the absorption spectra can be different. Unfortunately, the absorption spectra are not available and previous attempts to measure vis−NIR spectra of fullerene peapods were not successful since only bands of nanotube were found.[38] In addition the C_{60} fullerene does not require too large potentials to be reduced by the first electron (about −1.1 V vs ferrocene reference Fc/Fc^+ only) but a considerably higher driving force is required for the first oxidation (ca. 1.3 V vs Fc/Fc^+).[39] We have shown for DWCNTs that the potential applied to the outer wall is only partly transferred to the inner tube.[20,21,28,36] Hence, even a maximum magnitude of electrode potential (±1.5 V, which correspond to ca. +1.2 and −1.8 V vs Fc/Fc^+) applied in this study is not sufficient to oxidize fullerene to C_{60}^+. The reduction to C_{60}^- could be possible at our conditions with free molecules but, presumably, not with encapsulated ones. On the other hand it has been shown that encapsulated C_{60} interacts with near free electron states of SWCNTs. A hybridization between near free electron states of nanotubes and π-electron states of the fullerene[40] may facilitate the electron density redistribution between the nanotube wall and the fullerene. Furthermore, the fullerenes form a one-dimensional (albeit orientationally disordered) chain within the nanotube. Through the interaction with the nanotube wall, it is possible for charge transfer to occur such that the charge per fullerene corresponds to partial charging far less than a single electron. The electronic structure of thus doped $C_{60}^{\delta-}$ will be different from that of neutral C_{60}, and thus resonance effects may occur. The positive doping of a C_{60} cage during anodic charging of C_{60} peapods is also supported by the small upshift of the $A_g(2)$ mode observed at higher anodic potentials. Furthermore, the molecule of C_{60} belongs to the extremely symmetric icosahedral group I_h and its orbitals are highly degenerated; therefore the ionic states are accordingly subject to the nonadiabatic interaction. According to JT theorem the electronic degeneracy is distorted by the coupling of the electrons to some specific molecular vibrations (JT active) modes, so as to lift the degeneracy and lower the total energy. While we do not expect that a Jahn−Teller distortion occurs if the fullerenes are only charged by a fraction of electron, the change in electron−phonon coupling of the charged structure may nevertheless result in the enhancement of the Raman signal.

TABLE 1: Calculated A_g Modes of C_{60} and C_{60}^{5+} Using the B3LYP DFT Functional and the 6-311G Basis Set

	C_{60} freq (cm^{-1})	C_{60} int. (arb. u.)	C_{60}^{5+} freq (cm^{-1})	C_{60}^{5+} int. (arb. u.)
$A_g(1)$	491.3	136.8	488.3	236.6
$A_g(2)$	1501.9	521.1	1520.2	38.4

Theory

We have performed first principles density functional theory calculations to explain the experimentally observed intensity profile and frequency shifts. The calculations were performed with the Gaussian 03 package (Gaussian, Inc., Wallingford, CT, 2003), using the B3LYP functional and a large 6-311G basis set. We studied the effect of positive charging on the frequencies and intensities of the pinch and radial breathing modes.

As discussed earlier, while the screening effect of the nanotube allows only a small charge to penetrate the tube during electrochemical treatment, a small amount of charge should be present on the fullerenes nonetheless. We expect that the observed frequency shift is due to this charge, and therefore it should still be significant, possibly on the order of 0.1 e. Ideally, one would calculate the Raman spectrum of a C_{60} molecule with such a low charge; however, due to the limitations of Gaussian 03, only integer charges can be used in the calculation. There is another issue which must be considered, that is, Jahn−Teller distortion. It is well-known that single charged C_{60}^+ suffers Jahn−Teller distortion, which further complicates theoretical studies. For such a low charge as what we expect, there should be no Jahn−Teller distortion at all. Therefore, it is preferential to perform the calculation with quintuple positive charge on the fullerene instead of a single positive charge, in which case no Jahn−Teller distortion occurs. While this amount of charge is obviously not present in the experiment, it is necessary to ensure that Jahn−Teller distortion does not influence the results. The results obtained from this calculation can be used to interpolate to very low charging levels (which would be necessary even in the case of using a single positive charge), and by comparing the calculated frequency shifts with the experiments, we can make a theoretical estimate of the charge of the fullerenes.

Our DFT results are summarized in Table 1, along with the results on neutral C_{60}. As it can be seen, the frequency of the $A_g(2)$ mode shifts in the same direction as in the case of the experiment. The calculated shift is 18 cm^{-1}, which corresponds to an upshift of roughly 3.5 cm^{-1} per removed electron, a value similar to the roughly 6 cm^{-1} per added electron downshift that is known experimentally for negatively charged fullerenes in K_xC_{60}.[41] Assuming a linear dependence of the pinch

mode frequency as a function of the charge, we can now interpolate to the range of a few wavenumbers shift which is the typical magnitude of the shift seen in our measurements. The interpolation yields that an observed shift of $1-2$ cm^{-1} is consistent with a positive charge of $0.25-0.5$ e. This small charge value agrees with the expectation that only a very small charge can be accommodated on intratubular fullerenes.

As for the intensities, we found that the $A_g(2)$ mode intensity of charged fullerenes is significantly lower than that of neutral C_{60}, which is consistent with the decreasing trend seen in our measurements at the laser excitation of 1.16 eV. The good qualitative agreement between the calculations and the 1.16 eV measurements is due to the nonresonant nature of the spectrum at this laser energy. For the other laser excitation energies we used, the strong deviations and the generic increasing trend in the intensity suggest resonance effects as we discussed above, which are not taken into account in our calculation.

Conclusions

We have presented a detailed Raman in situ spectroelectrochemical study of C_{60} embedded inside SWCNTs. It is demonstrated for the $A_g(2)$ Raman mode, that the signal of C_{60} in peapods is dependent both on the electrode potential and also on the laser excitation energy. The $A_g(2)$ mode Raman intensity/potential profiles are shown for seven different laser excitation energies. While for negative electrode potentials we observed only bleaching of the Raman intensity of the $A_g(2)$ mode, for positive electrode potentials the development of the Raman intensity was strongly dependent on laser excitation energy. The decrease of intensity at positive electrode potential was found only for 1.16 eV laser excitation energy. For the other six probed laser excitation energies only enhancement of the $A_g(2)$ mode has been observed during anodic doping. The 2.54 eV laser excitation energy exhibited maximum enhancement at high positive potentials. For this excitation energy the intensity of the Raman signal of the $A_g(2)$ mode was about 2.5 times stronger at 1.5 V than at 0 V. First principles calculations have shown that the observed frequency shift is consistent with a charging of no more than $0.25-0.5$ e and that in the limit of nonresonant Raman scattering only bleaching is expected upon positively charging the fullerenes, and no intensity increase. Hence, it is suggested that the enhancement of the Raman signal of the $A_g(2)$ mode is not related to the changes of the electronic structure of the SWCNT but to the change of the resonant condition of the C_{60} fullerene caused by the excess charge.

Experimental Section

The electrodes for in situ spectroelectrochemical studies were fabricated by the evaporation of a sonicated ethanolic slurry of C_{60}@SWCNTs (available from our previous study[8]) on Pt electrodes. The film was outgassed at 80 °C in vacuum and then the electrode was mounted in the Raman spectroelectrochemical cell. The spectroelectrochemical cell was airtight, had a single-compartment, and was equipped with a glass optical window for spectroscopic measurements.

The cell was assembled in a glovebox (M. Braun); the glovebox atmosphere was N_2 containing <1 ppm of both O_2 and H_2O. Electrochemical experiments were carried out using Autolab PGSTAT 30 potentiostat with Pt auxiliary and Ag-wire pseudoreference electrodes, the electrolyte solution was 0.2 M $LiClO_4$ + acetonitrile (both from Aldrich; the latter dried by 4 Å molecular sieve). The Raman spectra were excited by 2.70, 2.60, 2.54, 2.41, 2.33 2.18 eV using mixed Ar^+/ Kr^+ laser (Innova 70C series, Coherent) and 1.16 eV laser (mpc 6000, Laser Quantum). Spectra were recorded by a Labram HR spectrometer (Horiba Jobin Yvon) interfaced to an Olympus BH2 microscope (objective 50×). The laser power impinging on the cell window or on the dry sample was between 1 and 5 mW. The spectrometer was calibrated by the F_{1g} mode of Si at 520.2 cm^{-1}.

Acknowledgment. This work was supported by the Academy of Sciences of the Czech Republic (Contracts IAA400400804, IAA400400911, and KAN200100801) and Czech Grant agency (203/07/J067, P204/10/1677), the OTKA in Hungary (Grants F68852 and K60576), and the Marie Curie IEF project NANOTRAN (PIEF-GA-2008-220094).

References and Notes

(1) Monthioux, M. Filling single-wall carbon nanotubes. *Carbon* **2002**, *40* (10), 1809–1823.

(2) Takenobu, T.; Takano, T.; Shiraishi, M.; Murakami, Y.; Ata, M.; Kataura, H.; Achiba, Y.; Iwasa, Y. Stable and controlled amphoteric doping by encapsulation of organic molecules inside carbon nanotubes. *Nat. Mater.* **2003**, *2* (10), 683–688.

(3) Sloan, J.; Novotny, M. C.; Bailey, S. R.; Brown, G.; Xu, C.; Williams, V. C.; Friedrichs, S.; Flahaut, E.; Callender, R. L.; York, A. P. E.; Coleman, K. S.; Green, M. L. H.; Dunin-Borkowski, R. E.; Hutchison, J. L. Two layer 4: 4 co-ordinated KI crystals grown within single walled carbon nanotubes. *Chem. Phys. Lett.* **2000**, *329* (1−2), 61–65.

(4) Kataura, H.; Maniwa, Y.; Kodama, T.; Kikuchi, K.; Hirahara, K.; Suenaga, K.; Iijima, S.; Suzuki, S.; Achiba, Y.; Kratschmer, W. High-yield fullerene encapsulation in single-wall carbon nanotubes. *Synth. Met.* **2001**, *121* (1−3), 1195–1196.

(5) Bandow, S.; Takizawa, M.; Hirahara, K.; Yudasaka, M.; Iijima, S. Raman scattering study of double-wall carbon nanotubes derived from the chains of fullerenes in single-wall carbon nanotubes. *Chem. Phys. Lett.* **2001**, *337* (1−3), 48–54.

(6) Xiu, P.; Zhou, B.; Wenpeng, Q.; Hangjun, L.; Yusong, T.; Haiping, F. Manipulating biomolecules with aqueous liquids confined within single-walled nanotubes. *J. Am. Chem. Soc.* **2009**, *131*, 2840–2845.

(7) Kavan, L.; Kalbac, M.; Zukalova, M.; Krause, M.; Dunsch, L.; Kataura, H. Redox doping of double-wall carbon nanotubes and C-60 peapods. *Fullerenes, Nanotubes, Carbon Nanostruct.* **2005**, *13*, 115–119.

(8) Kavan, L.; Dunsch, L.; Kataura, H.; Oshiyama, A.; Otani, M.; Okada, S. Electrochemical tuning of electronic structure of C-60 and C-70 fullerene peapods: In situ visible near-infrared and Raman study. *J. Phys. Chem. B* **2003**, *107* (31), 7666–7675.

(9) Kalbac, M.; Kavan, L.; Zukalova, M.; Dunsch, L. Doping C-60 fullerene peapods with lithium vapor: Raman spectroscopic and spectroelectrochemical studies. *Chem.—Eur. J.* **2008**, *14* (20), 6231–6236.

(10) Kalbac, M.; Kavan, L.; Zukalova, M.; Dunsch, L. Two positions of potassium in chemically doped C-60 peapods: An in situ spectroelectrochemical study. *J. Phys. Chem. B* **2004**, *108* (20), 6275–6280.

(11) Kalbac, M.; Kavan, L.; Zukalova, M.; Dunsch, L. Spectroelectrochemical Recognition of Chemical Dopants in the Inner Space of Carbon Nanostructures. *NANO* **2006**, *1*, 219–227.

(12) Kalbac, M.; Kavan, L.; Zukalova, M.; Dunsch, L. The influence of an extended fullerene cage: a study of chemical and electrochemical doping of C_{70} peapods by in situ Raman spectroelectrochemistry. *J. Phys. Chem. C* **2007**, *111*, 1079–1085.

(13) Sun, B. Y.; Sato, Y.; Suenaga, K.; Okazaki, T.; Kishi, N.; Sugai, T.; Bandow, S.; Iijima, S.; Shinohara, H. Entrapping of exohedral metallofullerenes in carbon nanotubes: (CsC60)(n)@SWNT nano-peapods. *J. Am. Chem. Soc.* **2005**, *127* (51), 17972–17973.

(14) Guan, L. H.; Suenaga, K.; Okazaki, T.; Shi, Z.; Gu, Z.; Iijima, S. Coalescence of C-60 molecules assisted by doped iodine inside carbon nanotubes. *J. Am. Chem. Soc.* **2007**, *129* (29), 8954–8955.

(15) Kavan, L.; Dunsch, L. Spectroelectrochemistry of carbon nanostructures. *ChemPhysChem* **2007**, *8* (7), 975–998.

(16) Holloway, A. F.; Toghill, K.; Wildgoose, G. G.; Compton, R. G.; Ward, M. A. H.; Tobias, G.; Llewellyn, S. A.; Ballesteros, B.; Green, M. L. H.; Crossley, A. Electrochemical opening of single-walled carbon nanotubes filled with metal halides and with closed ends. *J. Phys. Chem. C* **2008**, *112* (28), 10389–10397.

(17) Rafailov, P. M.; Thomsen, C.; Dettlaff-Weglikowska, U.; Roth, S. High Levels of Electrochemical Doping of Carbon Nanotubes: Evidence for a Transition from Double-Layer Charging to Intercalation and Functionalization. *J. Phys. Chem. B* **2008**, *112* (17), 5368–5373.

(18) Kalbac, M.; Kavan, L.; Dunsch, L. Changes in the Electronic States of Single Walled Carbon Nanotubes as Followed by a Raman Spectroelectrochemical Analysis of the Radial Breathing Mode. *J. Phys. Chem. C* **2008**, *112* (43), 16759–16763.

(19) Kalbac, M.; Kavan, L.; Dunsch, L.; Dresselhaus, M. S. Development of the tangential mode in the Raman spectra of SWCNT bundles during electrochemical charging. *Nano Lett.* **2008**, *8* (4), 1257–1264.

(20) Kalbac, M.; Kavan, L.; Zukalova, M.; Dunsch, L. In-situ Vis-NIR and Raman Spectroelectrochemistry of Double Wall Carbon Nanotubes. *Adv. Funct. Mater.* **2005**, *15*, 418–426.

(21) Kalbac, M.; Kavan, L.; Zukalova, M.; Dunsch, L. In situ Raman spectroetectrochemical study of C-13-Labeled fullerene peapods and carbon nanotubes. *Small* **2007**, *3*, 1746–1752.

(22) Kavan, L.; Dunsch, L. Ionic liquid for in situ Vis/NIR and Raman spectroelectrochemistry: Doping of carbon nanostructures. *ChemPhysChem* **2003**, *4* (9), 944–950.

(23) Kalbac, M.; Kavan, L.; Zukalova, M.; Yang, S. F.; Cech, J.; Roth, S.; Dunsch, L. The change of the state of an endohedral fullerene by encapsulation into SWCNT: A Raman spectroelectrochemical study of Dy3N@C-80 peapods. *Chem.—Eur. J.* **2007**, *13* (31), 8811–8817.

(24) Kvarnstrom, C.; Neugebauer, H.; Kuzmany, H.; Sitter, H.; Sariciftci, N. S. An in situ spectrochemical study of the reduction of thin fullerene films. *J. Electroanal. Chem.* **2001**, *511* (1−2), 13–19.

(25) Gallagher, S. H.; Armstrong, R. S.; Clucas, W. A.; Lay, P. A.; Reed, C. A. Resonance Raman scattering from solutions of C-60. *J. Phys. Chem. A* **1997**, *101* (16), 2960–2968.

(26) Mcglashen, M. L.; Blackwood, M. E.; Spiro, T. G. Resonance Raman Spectroelectrochemistry of the C60 Radical-Anion. *J. Am. Chem. Soc.* **1993**, *115* (5), 2074–2075.

(27) Reed, C. A.; Bolskar, R. D. Discrete fulleride anions and fullerenium cations. *Chem. Rev.* **2000**, *100* (3), 1075–1119.

(28) Kalbac, M.; Kavan, L.; Dunsch, L. In situ Raman spectroelectrochemistry as a tool for the differentiation of inner tubes of DWCNT and thin SWCNT. *Anal. Chem.* **2007**, *79*, 9074–9081.

(29) Joung, S. K.; Okazaki, T.; Kishi, N.; Okada, S.; Bandow, S.; Iijima, S. Effect of Fullerene Encapsulation on Radial Vibrational Breathing-Mode Frequencies of Single-Wall Carbon Nanotubes. *Phys. Rev. Lett.* **2009**, *103* (2), 027403−027403−4.

(30) Corio, P.; Santos, P. S.; Brar, V. W.; Samsonidze, G. G.; Chou, S. G.; Dresselhaus, M. S. Potential dependent surface Raman spectroscopy of single wall carbon nanotube films on platinum electrodes. *Chem. Phys. Lett.* **2003**, *370* (5−6), 675–682.

(31) Kalbac, M.; Farhat, H.; Kavan, L.; Kong, J.; Sasaki, K.; Saito, R.; Dresselhaus, M. S. Electrochemical charging of individual single-walled carbon nanotubes. *ACS Nano* **2009**, *3* (8), 2320–2328.

(32) Kalbac, M.; Kavan, L. The Influence of the Resonant Electronic Transition on the Intensity of the Raman Radial Breathing Mode of Single Walled Carbon Nanotubes during Electrochemical Charging. *J. Phys. Chem. C* **2009**, *113*, 16408–16413.

(33) Kavan, L.; Janda, P.; Krause, M.; Ziegs, F.; Dunsch, L. Rotating Cell for in Situ Raman Spectroelectrochemical Studies of Photosensitive Redox Systems. *Anal. Chem.* **2009**, *81* (5), 2017–2021.

(34) Pichler, T.; Kuzmany, H.; Kataura, H.; Achiba, Y. Metallic polymers of C-60 inside single-walled carbon nanotubes. *Phys. Rev. Lett.* **2001**, *87* (26), 267401−267401−4.

(35) Pfeiffer, R.; Kuzmany, H.; Pichler, T.; Kataura, H.; Achiba, Y.; Melle-Franco, M.; Zerbetto, F. Electronic and mechanical coupling between guest and host in carbon peapods. *Phys. Rev. B* **2004**, *69* (3), 035404–035404-7.

(36) Kalbac, M.; Green, A. A.; Hersam, M. C.; Kavan, L. Tuning of Sorted Double-walled Carbon Nanotubes by Electrochemical Charging. *ACS Nano* DOI: 10.1021/nn900895w.

(37) Canton, S. E.; Yencha, A. J.; Kukk, E.; Bozek, J. D.; Lopes, M. C. A.; Snell, G.; Berrah, N. Experimental evidence of a dynamic Jahn-Teller effect in C-60 (+). *Phys. Rev. Lett.* **2002**, *89* (4), 045502–045502-4.

(38) Kavan, L.; Dunsch, L.; Kataura, H. In situ Vis-NIR and Raman spectroelectrochemistry at fullerene peapods. *Chem. Phys. Lett.* **2002**, *361* (1−2), 79–85.

(39) Bruno, C.; Doubitski, I.; Marcaccio, M.; Paolucci, F.; Paolucci, D.; Zaopo, A. Electrochemical generation of C-60(2+) and C-60(3+). *J. Am. Chem. Soc.* **2003**, *125* (51), 15738–15739.

(40) Okada, S.; Otani, M.; Oshiyama, A. Electron-state control of carbon nanotubes by space and encapsulated fullerenes. *Phys. Rev. B* **2003**, *67* (20), 205411–205411-5.

(41) Pichler, T.; Matus, M.; Kurti, J.; Kuzmany, H. Phase separation in KxC-60 (0-less -than-or-equal-to-x-less-than -or-equal-to-6) as obtained from in situ Raman spectroscopy. *Phys. Rev. B* **1992**, *45* (23), 13841–13844.

JP9103273